Revista Ciência Agronômica, v. 57, e202494376, 2026
Centro de Ciências Agrárias - Universidade Federal do Ceará, Fortaleza, CE
www.ccarevista.ufc.br

RESEARCH ARTICLE
ISSN 1806-6690

Soil water content measurement by capacitance technique: sensor design and performance[1]

Gabriela Rodrigues da Costa[2], Marinaldo Ferreira Pinto[3], Jaídson Gonçalves da Rocha[3], Celita Nathalia Vasconcelos Perdigão[4], Daniel Fonseca de Carvalho[3]*

ABSTRACT - Soil water content is an important variable in irrigation management and can be determined by using electronic sensors. This study aimed to develop a capacitive sensor and evaluate its performance in soil/substrate materials. Prototypes of sensors with parallel and coplanar plates were developed, using different printed circuit boards and insulating materials. In an initial evaluation, the coplanar sensor (CPS) built out of fiberglass board and insulated with varnish showed greater sensitivity in estimating soil moisture, and easier construction. The performance of the CPS was compared to that of the commercial 5TE sensor from Decagon Devices (CS), after calibrating them on different soil/substrate materials contained in PCV columns. At this stage, measurements of volumetric water content (θ) obtained by monitoring the masses of pots on precision scales were compared to sensors readings, generating regression models relating θ to period (CPS) and permittivity (CS). The estimated θ values were compared to the measured values and evaluated by performance indices. The sensitivity of CPS to salinity and temperature was further evaluated in water for the range of 0.5 to 3.0 dS m^{-1}, and 15 to 40 °C, respectively. The developed sensor had low manufacturing cost (US$ 4.13) and satisfactory performance, with a maximum mean absolute error of 0.0178 cm^3 cm^{-3}, and less sensitivity (9.9%) than CS (34.2%) in relation to salinity. Both sensors showed a variation of approximately 15% for a temperature variation of 15 to 40 °C.

Key words: Irrigation management. Soil moisture. Soil permittivity.

INTRODUCTION

Water management in irrigation systems consists of determining and supplying the amount of water needed for the full development of crops, aiming to maximize productivity or net income. Soil water content is one of the most important variables to be monitored to allow the rational use of water in agriculture (Vories; Sudduth, 2021).

Water plays an important role in solubilizing and making soil nutrients available to plants (Verma; Pahuja, 2021) and, therefore, the occurrence of prolonged dry periods causes damage to crop development, sometimes leading to total production loss (Oduor *et al*., 2021). Thus, technologies that monitor soil moisture in real time contribute to the efficient management of water balance in agricultural production systems (Leone, 2022; Roth *et al*., 1990; Yu *et al*., 2021), and also in practices such as fertilization, soil preparation, and the selection of more efficient cropping systems that promote greater efficiency in natural resource use and a reduction in environmental impacts (Zhang *et al*., 2024).

In addition to supporting agricultural practices, continuous monitoring of soil water dynamics provides essential information for decision-making regarding natural resource conservation, agricultural planning, and the assessment of climate change impacts (Duarte; Hernandez, 2024). Soil water content is a key variable in quantifying hydrological processes such as infiltration, water redistribution within the soil profile, deep drainage, surface runoff, and aquifer recharge (Vereecken *et al*., 2022), and assessment landslide (Badavath *et al*., 2024); it also influences evapotranspiration fluxes, cloud formation, the development of extreme events, and regional precipitation patterns, and is widely used in meteorological, climate, and hydrological forecasting models (Liu *et al*., 2023; Zeng *et al*., 2023).

DOI: 10.5935/1806-6690.v57e202494376
Section Editor: Prof. Everton Alves Rodrigues Pinheiro - pinheiroear@mail.uft.edu.br
Author for correspondence
Received for publication in 21/10/2024: approved in 29/07/2026
[1]Part of the first author's Master's thesis, submitted to the Graduate Program in Agronomy – Soil Science
[2]Graduate Program in Agronomy, Soil Science, Seropédica-RJ, Brazil, gabirodrigues.ufrrj@gmail.com (ORCID ID 0000-0001-9544-4947)
[3]Department of Engineering, Institute of Technology, Federal Rural University of Rio de Janeiro, Seropédica-RJ, Brazil, mfpufrrj@yahoo.com.br (ORCID ID 0000-0002-9368-6122), jaidsongr@gmail.com (0000-0002-9933-526X), daniel.fonseca.carvalho@gmail.com (ORCID ID 0000-0001-7629-9465)
[4]Institute of Agronomy, Federal Rural University of Rio de Janeiro, Seropédica-RJ, Brazil, celitaperdigao@gmail.com (ORCID ID 0000-0001-6167-1324)

There are different methodologies for quantifying soil water content, such as tensiometry (Cardenas-Lailhacar; Dukes, 2010), neutron moderation (Heistermann *et al*., 2024), time domain reflectometry (TDR) (Singh *et al*., 2023), frequency domain reflectometry (FDR) (Zhang *et al*., 2024), among others. All of them have potential and limitations of use and therefore must be adopted carefully. Different from TDR probes, which are costly (Songara; Patel, 2022), capacitive sensors (FDR) have been widely popularized in recent decades due to their ease of reading and their non-destructive measurements (Oliveira *et al*., 2020). The operating principle of the FDR is the variation of the dielectric permittivity of the medium in response to the water content (Sharma *et al*., 2017), offering simplicity in terms of handling for in-situ measurements.

Electronic soil moisture sensors pave the way toward automation, more intensive monitoring of irrigation systems and obtaining highly detailed experimental data, allowing for more accurate and reliable information. This is especially valid when digital technologies that can create tools to implement agriculture 4.0 are combined (Kamienski; Visoli, 2018).

Taking this into account, it is essential to master the technology of building sensors for monitoring soil moisture and expand accessible technologies for agriculture. Therefore, this study aimed to develop a low-cost capacitive sensor for water content determination and to compare its performance to that of a commercial sensor in different soil/substrate materials.

MATERIAL AND METHODS

Sensor development

The capacitive sensor was designed to be 14 cm long and 3 cm wide, with the electronic circuit positioned at the top and the capacitive sensor at the base. Initially, two types of capacitors (parallel plate-PPS and coplanar-CPS) were evaluated in different printed circuit boards and insulating materials, both covered with a copper layer. The sensing electrodes were then formed by chemically etching the copper layer to produce the desired electrode geometry and circuit tracks. The distances between the capacitor plates in the CPS and PPS sensors were, respectively, 1.0 and 17.0 mm. Initially, the CPS was made of fiberglass with a varnish coating to insulate the electronic circuits (Implastec), and of Phenolite™ coated with heat shrink tubing. The PPS was made only in Phenolite™, coated with a heat shrink tubing. To facilitate the installation of this sensor (PPS), a porous plate was used as the dielectric medium, aiming to eliminate signal interference caused by the physical and chemical characteristics of the soil.

The initial design of the electronic sensor circuit was developed using the KiCad software. The electronic circuit is composed of the TLC555 oscillator in astable mode to convert capacitance into frequency (Eq. 1).

$$f = \frac{1.44}{C(R_1 + 2R_2)} \quad (1)$$

Where f is the output frequency (kHz), R_1 is the charging resistor (10 k), R_2 is the discharge resistor (100 k), and C is the capacitance measured (μF), which varies according to soil water content. After the circuit design was completed, the sensor's electronic circuit was printed on photographic paper and transferred to the copper plate using a thermal press (Figure 1).

The Phenolite™ plate was cut to the same dimensions as the drawing. For the etching process, the plate was immersed in a ferric chloride solution ($FeCl_3$) for approximately 15 min to remove the exposed copper surface, leaving only the electrode and circuit defined by the printed design. After corrosion, the plates were cleaned with an isopropyl alcohol solution to remove surface contaminants.

The process of insulating the varnish-based sensors was performed by immersion and then exposure to ambient conditions to dry for 72 h (Figure 2A). In the insulation with heat shrink tubing, the electrodes were inserted into a tube with a diameter of 20 mm, which adhered perfectly to the sensor plate using a thermal dryer (Figure 2B, C). After the insulation step, the electronic circuit components were soldered.

Figure 1 - Schematic drawing of coplanar (A) and parallel plate (B) capacitive sensors

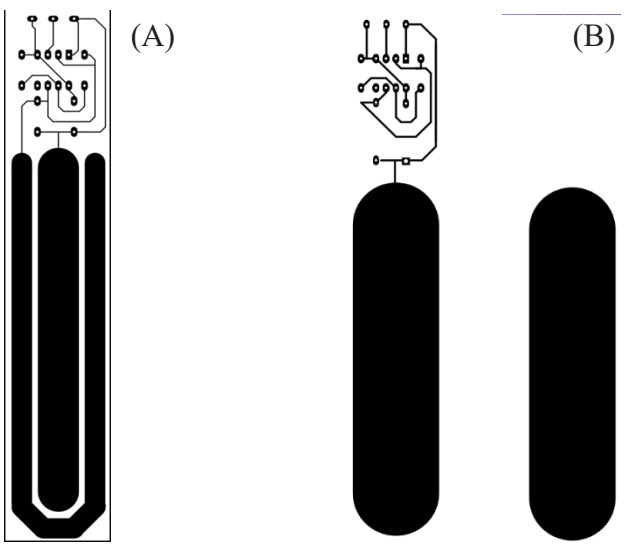

Figure 2 - Coplanar fiberglass sensor with varnish insulation (A) and plate sensor and heat shrink tubing coating: side view (B) and front view (C)

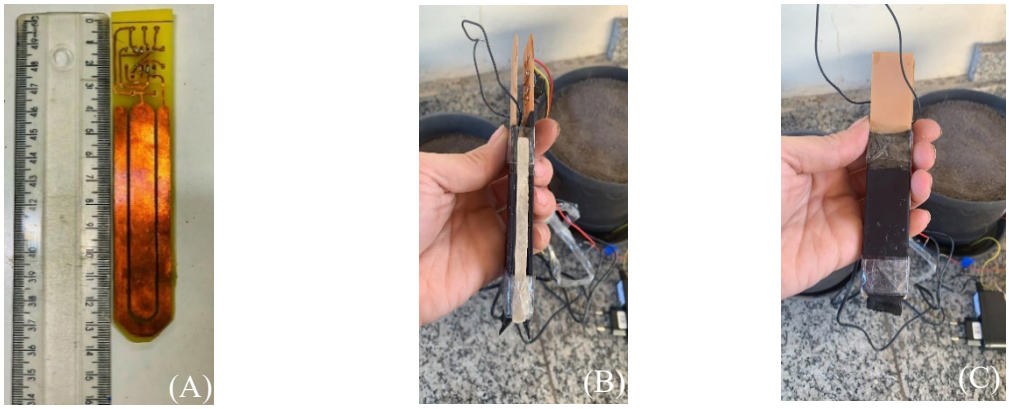

Evaluating the materials used and the sensor sensitivity to soil water content

Before evaluating sensitivity to soil water content, the electrical isolation of all coplanar sensors was evaluated. To do this, the sensor was immersed in water and then the electrical resistance was measured between the sensor plates. Insulation was considered adequate when the multimeter indicated infinite electrical resistance.

For assessing the sensitivity of the capacitor plates to water content variations, the sensors were inserted vertically in columns made of PVC pipe (100 mm - nominal diameter, 150.0 mm – height and useful volume of 2.0 L), filled with soil material classified as Ultisol. The columns were covered at the bottom with a nylon net (approximately 1.2 mm in diameter). Initially, the columns were saturated by immersion for 48 h and then placed on load cells, starting sensor readings using a digital multimeter. The evaluation period was from 06/15/2021 to 07/16/2021, and the sensor signals were collected at 7:30 am, 12:00 pm and 6:00 pm. Furthermore, mass readings were taken (soil column + sensor) on a precision scale. The volumetric water content of the soil columns was determined by the product of the gravimetric moisture by the previously determined soil bulk density.

The developed sensors' sensitivity was calculated between variations in frequency signal and the volumetric water content. The CPS developed in fiberglass and with varnish showed insulation sensitivity of 0.1% of water content at each frequency variation of 1.0 kHz. The same result was found for the PPS. In the CPS developed in Phenolite™, with insulation and anti-corrosive protection in heat shrink tubing, the sensitivity was 0.2%. In all sensors evaluated, the standard error was 0.01%. Based on the sensitivity presented and the ease of construction, the CPS model developed in fiberglass was chosen for performance evaluations and comparison with a commercial sensor.

Electronic circuit encapsulation and cost of materials

After defining the geometry and materials to make the sensor, the circuit was encapsulated, which serves as a physical protection of the electronic components against humidity and other environmental factors that could damage the circuit. Using silicone molds (Redecenter, PS) built with compatible dimensions to protect the sensor components (Figure 3A), the electronic circuit was protected with black epoxy resin (Redecenter, SQ-2119) and hardener (Redecenter, 3154), at a proportion of 3:1, which offered good resistance and finishing (Figure 3B). In the end, all costs for manufacturing the sensor and a reading device were calculated.

Performance of the developed sensor in different soil types and substrates

The evaluation process was carried out in 2 stages: calibrating the coplanar sensor developed (CPS) and 5TE commercial sensor (CS) (Decagon Devices, Inc., Pullman, WA, USA) in different soil/substrate materials; and comparing their performance and accuracy in determining the water content. The sensors were evaluated on 4 types of soil/substrate materials: biosolids (stabilized sewage sludge), sandy texture from the surface horizon of an *Argissolo Vermelho Amarelo* (Ultisol) (SI), medium texture of a transitional horizon of an *Argissolo Amarelo* (Ultisol) (SII), clayey texture from the Bt horizon of an *Argissolo Vermelho* (Ultisol) (SIII), collected on the Federal Rural University of Rio de Janeiro (UFRRJ) campus. The particle-size distribution of the materials is shown in Table 1.

The water retention curves in the materials were determined by the simplified evaporation method, using the commercial equipment Hyprop® (Pertassek *et al*., 2015) and fitted with the van Genuchten model (Eq. 2), whose parameters are presented in Table 1. This device evaluates the water content in the material at equilibrium with a matric

potential (of up to approximately -80 kPa, which corresponds to the expected soil water content range for most agricultural crops (Rotimi *et al*., 2015).

$$\theta = \theta r + \frac{\theta s - \theta r}{\left[1 + (\propto \psi)^n\right]^m} \quad) \tag{2}$$

where θ_r is residual water content; θ_s is saturation water content; and α, "n" and "m" are equation fitting parameters.

To calibrate and compare the developed sensors, 10 pots with a capacity of 3.0 L were used, for each type of soil/substrate, filled with 2.0 L of sieved material and dried in an oven for 48 h at 105 ºC. The material volume was determined using a graduated cylinder, and the weights of filled pots were obtained using a precision scale. Then, the pots were saturated for 24 h.

After the saturation period, the pots were removed from the tray so that the excess water could be drained. After installing the sensors in the pots, in the vertical position, data collection began, using 5 pots for the CPS and 5 for the CS.

Data collection, reading and storage environment

The sensor signals were measured in an air-conditioned environment at temperature of 23 °C and the pots were under constant lighting from halogen lamps to accelerate evaporation in the soil/substrate materials, due to the increase in temperature near the pots. The water content variation in the pots was also influenced by the low relative humidity imposed by the environment's climate control.

The mass readings in pots containing the CPS were obtained using scales built with a load cell (capacity of 5.0 kg), while in the pots with the CS mass readings were performed using a commercial precision scale (capacity of 5.0 kg ± 0.01 g) (Marte AD 5002). The scales for evaluating the CPS were built aiming to optimize data collection and obtain a greater number of sensor readings, thus detecting the mass variation due to evaporation from the soil/substrate materials during the drying process.

Scale calibration was carried out through 5 loading and unloading cycles of known masses (75 g) on the pots, making it possible to calculate the mass in response to the load cell signal variation. The value estimated by the module was related to the actual mass added to obtain the calibration curve. To minimize creep, hysteresis, and long-term drift under sustained load conditions, the load cells were kept under controlled laboratory conditions and recalibrated before each measurement cycle throughout the entire data collection period. The calibration equation was obtained through linear regression, resulting in a mean standard deviation of 0.66 g and R^2 of 0.9998.

Figure 3 - Side (A) and upper (B) views of the constructed silicone mold and coplanar sensor with varnish-based insulation and resin encapsulation of the electrical circuit (C)

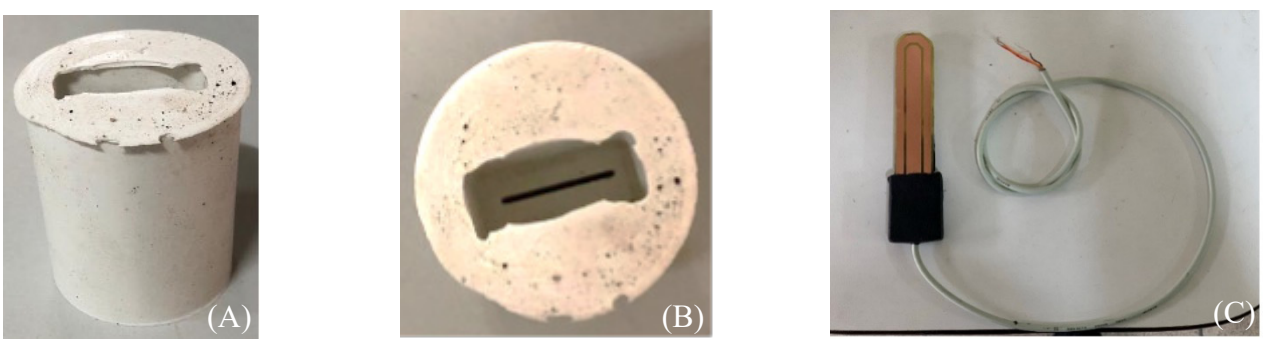

Table 1 - Particle-size composition of the soils/substrate used to calibrate the capacitive sensor

Soil/substrate materials	Total sand (%)	Silt (%)	Clay (%)	θr	θs	α (cm^{-1})	n**	m**
	(0.05 to 2 mm)	(0.002 to 0.05 mm)	(< 0.002 mm)	(cm^3 cm^{-3})				
Biosolid	76.1*	23.9*	-	0.043	0.74	0.0874	1.537	0.999
Soil I (SI)	83.0	4.0	13.0	0.033	0.36	0.0224	1.8796	0.2272
Soil II (SII)	57.0	9.0	34.0	0.066	0.41	0.1189	1.9027	0.2692
Soil III (SIII)	31.0	23.0	46.0	0.079	0.42	0.4193	1.9517	1.1798

*granulometric classification corresponding to the particle size of the sand or silt fractions, **model fitting parameters

Table 2 - Models fitted between volumetric water content values (y, in cm3 cm-3) and period (x, in ms) on the coplanar sensor (CPS), or permittivity (x, in F m-1) on the commercial sensor (CS)

Soil/substrate materials	Sensor	Pots	Parameters of the selected model ($y = a_1 + a_2x + a_3x^2$)			P*	R^{2**}
			a1	a2	a3		
Biosolid	CPS	P1	-0.0023	-3.9584	704.0010	2.200 x 10-16	0.9876
		P2	-0.1119	11.5691	661.0633	9.504 x 10-14	0.9735
		P3	-0.1937	19.3942	558.2083	1.637 x 10-14	0.9787
		P4	-0.1795	36.2300	-789.3422	4.870 x 10-11	0.9701
		P5	-0.1990	28.7846	-429.6566	5.071 x 10-16	0.9925
	CS	P1	-0.0494	2.846 x 10-5	-	2.200 x 10-16	0.9889
		P2	-0.0452	2.944 x 10-5	-	2.200 x 10-16	0.9849
		P3	-0.0268	2.842 x 10-5	-	1.543 x 10-10	0.9102
		P4	-0.0426	4.303 x 10-5	-	1.642 x 10-13	0.9518
		P5	-0.0730	2.022 x 10-5	-	3.857 x 10-16	0.9846
SI	CPS	P1	0.4883	-88.1315	4955.2359	5.135 x 10-8	0.9582
		P2	0.2889	-47.4684	2947.0117	2.142 x 10-7	0.9597
		P3	1.2047	-224.5812	11465.8685	3.181 x 10-6	0.9266
		P4	1.9903	-424.5334	23717.8050	4.969 x 10-6	0.9190
		P5	0.2821	-46.1389	2241.9322	2.012 x 10-9	0.9690
	CS	P1	0.0620	2.430 x 10-5	-	3.028 x 10-4	0.9283
		P2	0.0678	2.426 x 10-5	-	2.582 x 10-4	0.9327
		P3	0.0293	3.592 x 10-5	-	2.06 x 10-4	0.9531
		P4	0.0484	2.576 x 10-5	-	2.858 x 10-5	0.9188
		P5	0.0439	1.930 x 10-5	-	4.287 x 10-6	0.9526
SII	CPS	P1	1.2622	-214.0417	9871.6127	2.976 x 10-6	0.8601
		P2	0.1432	-11.2897	806.2631	3.477 x 10-6	0.9029
		P3	2.0573	-340.0677	14865.2341	2.421 x 10-6	0.8648
		P4	0.1335	-19.5824	1741.8951	2.468 x 10-9	0.9453
		P5	1.8863	-401.9309	22427.8799	2.539 x 10-5	0.8000
	CS	P1	0.0133	2.603 x 10-5	-	2.200 x 10-16	0.9931
		P2	0.0012	2.526 x 10-5	-	9.634 x 10-15	0.9867
		P3	0.0129	2.540 x 10-5	-	5.206 x 10-14	0.9877
		P4	0.0012	2.732 x 10-5	-	3.167 x 10-13	0.9838
		P5	-0.0288	2.203 x 10-5	-	3.821 x 10-12	0.9762
SIII	CPS	P1	4.8501	-979.9387	50680.5069	1.028 x 10-4	0.8412
		P2	7.2386	-1400.7723	68534.3220	1.181 x 10-7	0.9506
		P3	4.9655	-1027.9057	54275.1232	1.255 x 10-11	0.9921
		P4	4.6010	-1234.5091	84464.8162	6.283 x 10-8	0.9420
		P5	3.1679	-781.6434	49612.5894	3.199 x 10-8	0.9487
	CS	P1	-0.0085	3.912 x 10-5	-	4.933 x 10-10	0.9872
		P2	0.0105	3.808 x 10-5	-	3.342 x 10-12	0.9926
		P3	0.0212	3.117 x 10-5	-	1.023 x 10-12	0.9942
		P4	0.0226	2.888 x 10-5	-	2.200 x 10-16	0.9988
		P5	0.0132	1.844 x 10-5	-	5.632 x 10-11	0.9806

*probability level and **coefficient of determination

Data collection was carried out from 12/20/2021 to 05/13/2022, for the 4 types of soil/substrate materials. The signal readings provided by the CPS (period) were performed until the water content was less than 0.1 cm^3 cm^{-3} or matric potential was less than 100 kPa.

To collect and store data from sensors and load cells, two Arduino Mega 2560 boards were used. One board (secondary board) was responsible for receiving the signal from the developed sensors and transmitting it via serial communication to a second board (main board). The main board was used to carry out load cell readings, using the HX-711 signal amplification module, receive the data from the secondary board, and store both datasets on a microSD card (SD-SPI module) as text files (txt) (Sharma *et al*., 2017). As for the CS, permittivity readings of the medium obtained were performed daily, at 08:00 am, using the ProCheck reading interface (Decagon Devices, Pulman, WA). To ensure a direct comparison between the developed sensor and CS, only measurements acquired at 8 am in both sensors were used for the comparative analyses.

Performance evaluation of sensors (CPS and CS) in different soil/substrate materials

For each soil/substrate material and sensors evaluated, sensor calibration curves were determined using linear regression, with a second-degree polynomial for the SD sensors and a first-degree polynomial for the CS sensors (Table 2). Verma and Pahuja (2021) also observed improvements in accuracy using a capacitive sensor when fitting soil moisture variation using a second-degree polynomial. Based on the calibration curves of each sensor and the value of the measured signal, the soil moisture estimated by the sensors was calculated and compared with measurements determined by the gravimetric method.

The water content values obtained (θ_e) were correlated with the water content values determined by the gravimetric method (θ_d) in the soil/substrate materials, and evaluated by the Willmott's agreement index (d), coefficient of determination (R^2), performance index (c) and percentage bias (PBIAS) (Moriasi *et al*., 2007). In addition, the mean absolute errors of the highest quartile, referring to the differences in readings between θ_d and θ_e, were subjected to Fisher's F test and analyzed at a 5% significance level.

In order to evaluate the effect of salinity on the sensors' signal, electrical conductivity (EC) tests were performed in deionized water, with different concentrations of potassium chloride (KCl) (3 molar), according to Zabolotnyi and Koshevoi (2020). Thus, the 3 sensors (CPS) and (CS) were analyzed in a range of 0.5 – 3.0 dS m^{-1}, obtained by adding 3.5 mL of KCl for an EC variation of approximately 1.0 dS m^{-1}. The solution and sensor set were placed on a magnetic stirrer to homogenize the solution and, after each addition of salt, EC measurements were performed using a digital conductivity meter.

Five repetitions were performed. The sensor was attached to an iron rod and completely immersed in a 1.0 L beaker with the solution.

Evaluating the sensitivity to salinity and temperature

To evaluate the behavior of the signal at different temperatures, the sensor was submerged in distilled water under a heated magnetic stirrer. The temperature was determined using a thermometer placed inside the liquid. Using the same fixture structure and data reading used in the EC test, the signal reading was performed every 5.0 °C increase in water temperature, evaluating the range of 15 to 40 °C.

RESULTS AND DISCUSSION

Performance evaluation of sensors (CPS and CS) in different soil/substrate materials

The CPS frequency variations were 25.5, 20.0 and 9.1 kHz per 0.1 cm^3 cm^{-3} for SI (sandy texture), SII (medium texture), SIII (clayey texture), respectively, and the maximum variation was observed in the biosolid, with an amplitude of 34.5 kHz per 0.1 cm^3 cm^{-3} (Figure 4).

Figure 4 - Sensitivity of the developed (CPS) sensor, for biosolid, sandy (SI), medium (SII) and clayey (SIII) textured soil materials

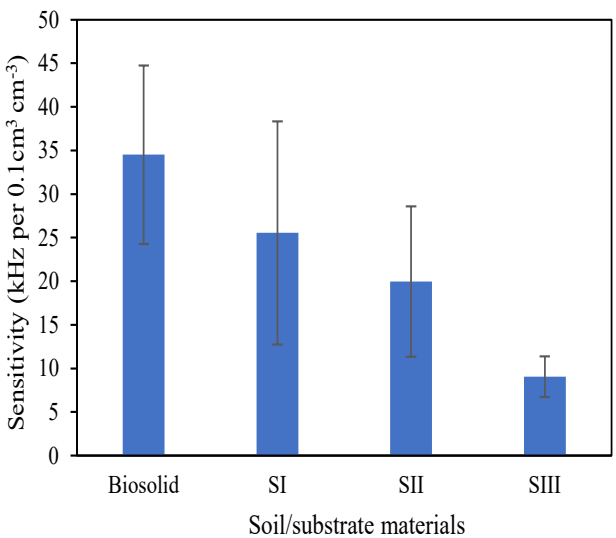

The response of the CPS signal can be explained by the particle sizes in the different types of soil/substrate materials used. The biosolid has more than 75% of its composition with particles between 0.05 and 2.0 mm, and, consequently, a smaller specific surface. On the other hand, 69% of the SIII material particles had an average diameter of less than 0.05 mm, of which 46% had an average diameter of less than 0.002 mm.

It should be noted that despite having a higher organic matter (OM) content, a characteristic that improves soil water retention, water retention at -80 kPa in the biosolid was lower than in the other materials analyzed, providing a greater range between the initial (θ_s) and end values of θ. The ability of OM to retain moisture reduces the fraction of free water in the soil, and the lower density observed in these substrates also leads to a decrease in soil permittivity (Szyplowska *et al*., 2021). As a result, it showed the largest variation in the volumetric water content (θ) during the drying process. Therefore, due to the characteristics of this substrate, the frequency variation as a function of substrate water content was greater than in other soil materials.

The evaluated sensors were able to estimate the water content in the different materials satisfactorily, with agreement indexes (d) above 0.98, coefficient of determination (R^2) above 0.94 and performance index (c) above 0.94 (Figure 5).

Figure 5 - Correlation analysis between the moisture values determined (θ_d) and estimated (θ_e) by the fitted models using the developed (CPS) and commercial (CS) sensor, for biosolid (A) and sandy (SI) (B), medium (SII) (C) and clayey (SIII) textured soil materials (D)

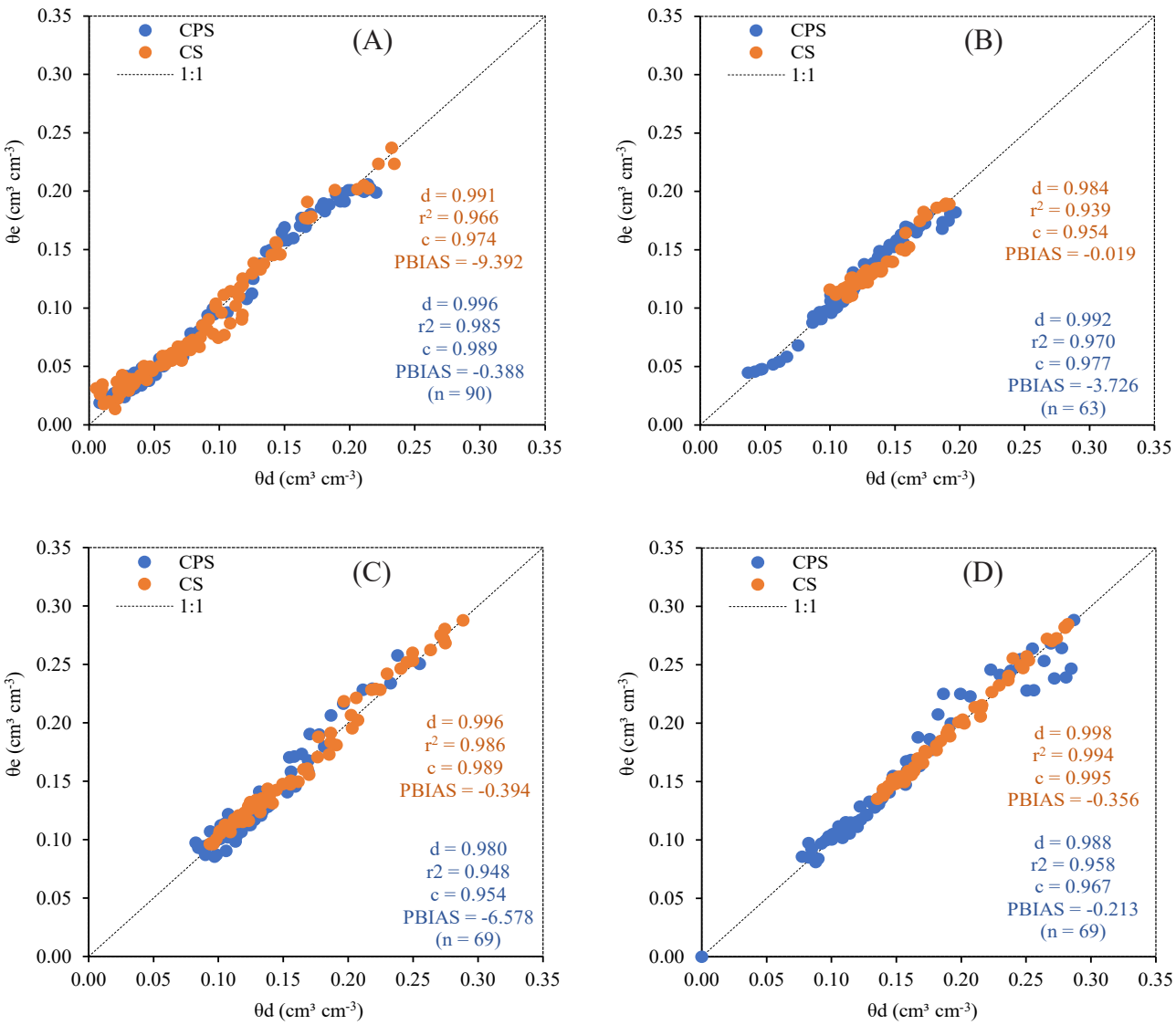

d – Willmott's agreement index; R^2 - coefficient of determination; c - performance index; PBIAS - percentage bias

For all the soil/substrate materials evaluated, the sensors indicated overestimation, with percentage bias (PBIAS) values ranging from -9.392 (CS in biosolids) to -0.019 (CS in soil I). PBIAS indicates the average tendency of simulated data to be greater or lower than that observed, with positive values indicating underestimation and negative values, overestimation of the data (Moriasi *et al*., 2007).

In the analyzed soil materials (Figures 5B, 5C and 5D), a gradual increase can be observed in the relative dispersion of the CPS signal, with the greatest dispersion in SIII. In finer grained soils, a water film forms around the soil particles, affecting the rotational freedom of the water molecule and decreasing the dielectric field of the medium, whose magnitude depends directly on the specific surface and the electric charge of the particle (Roth *et al*., 1990). The formation of this film can generate overestimation errors in soil moisture, leading to readings of lower values in the dielectric field of the medium in fine textured soils compared to coarser textured ones. This result can be confirmed by the value of the PBIAS index, which indicates overestimation errors in the CPS in medium textured soil. The greatest data dispersion in the CS signal occurred in soil materials SI (Figure 5B) and SII (Figure 5C), while for CS, the worst results among all sensors was observed in biosolid (Figure 5A) and soil materials SI (Figure 5B), which have larger particle size and, therefore, less contact with the sensor.

Clay activity is also a feature that influences the capacitive sensor signal. Soil shrinkage and expansion movements, due to clay activity, can affect moisture reading through the formation of a gas-sensor interface. Singh *et al*. (2018) observed that the greatest errors in measuring soil moisture using capacitive probes occurred under conditions with higher clay content and in soils with 2:1 clay (smectite).

Errors in estimating soil/substrate moisture values may occur due to interference in sensors caused by soil texture, chemical and physical properties, temperature and soil salinity (Topp *et al*., 1980). Using sensors with a measurement frequency below 100 MHz, Bogena *et al*. (2007) and Topp *et al*. (1980) observed that the dielectric constant was affected by soil particle size, leading to measurement errors. Roth *et al*. (1990) observed that soil porosity directly interferes with the dielectric constant, which may lead to errors in measuring soil moisture. The CPS operates in an operating range of less than 1.0 MHz, which may be another characteristic responsible for signal dispersion among soil materials with higher clay content. The CS reacts in frequency bands around 70 MHz, and in the SIII and in the biosolid, larger errors were observed than those observed in the CPS, as well as PBIAS, which indicated a greater tendency of CS data overestimation in the biosolid. Therefore, the results obtained by the CS demonstrate that, even operating in a higher frequency range than the CPS, in-situ calibration is still necessary for more accurate results.

The effectiveness of using capacitive sensors to determine moisture has been evaluated in different soil types and land use systems. The results obtained in this study are consistent with previous reports. Lo *et al*. (2020) worked on a mineral soil of medium texture under corn-soybean rotation in no-tillage, Gomes *et al*. (2017) in a medium textured Ferrudox and Pizetta *et al*. (2017) in a Typic Hapludalf, Typic Hapludox and an Oxisol, identifying R^2 greater than 0.90 after calibration, in agreement with the results found in this study. It is worth noting that the proposed sensor combines a low-cost and easy-to-fabricate design with an automated data acquisition system. In addition, its performance was evaluated not only in mineral soil materials with contrasting textures and chemical characteristics, but also in organic substrate, demonstrating its applicability in multiple substrates, with different hydraulic and dielectric properties.

The performance of the CPS and CS sensors did not show a statistically significant difference in terms of the absolute error of the lowest quartile for biosolids, SI and SII. There was a significant difference between the sensors for the mean absolute error of the highest quartile only for soil III (clayey) (0.0178 cm^3 cm^{-3}) (Table 3). In general, even with the difference observed between the sensors, both worked satisfactorily, showing error less than 2% in determining the soil water content.

Evaluating sensitivity to salinity and temperature

The sensor signals varied proportionally to the increase in electrical conductivity (from 0.5 to 3.0 dS m^{-1}) (Figure 6A), with 9.9% for CPS and 34.2% for CS. Although these variations do not directly correspond to changes in soil EC, since the evaluations were conducted in water, which has a different dielectric constant than soil, the results allow for a comparison of sensor performance, indicating that the CPS has lower sensitivity to salinity. Regarding temperature variation, both CPS and CS sensors showed a variation of approximately 15% for a temperature variation of 15 to 40 °C, with no statistical differences for all temperatures evaluated, that is, the sensors showed similar behavior (Figure 6B).

It should be noted that analyses of signal variation in response to variations in electrical conductivity such as temperature do not represent real field/soil conditions, serving only as a comparison between sensors and demonstrating the sensitivity of sensors to these factors. In soils, the variations would be different, since the physical hydraulic and dielectric properties of the soil also influence final sensor response.

Table 3 - Mean absolute error of the highest quartile between moisture values ($cm^3\ cm^{-3}$) obtained by the developed (CPS) and commercial (CS) sensors, for the different soil/substrate materials

Soil/substrate materials	Sensor		P-value
	CPS	CS	
Biosolid	0.0117	0.0150	0.3891
SI	0.0089	0.0070	0.1259
SII	0.0135	0.0105	0.1016
SIII	0.0178	0.0045	0.0032*

*significant at 5% probability level

Figure 6 - Sensitivity of the developed sensor (CPS) and commercial sensor (CS) to the increase in electrical conductivity (A) and temperature (B)

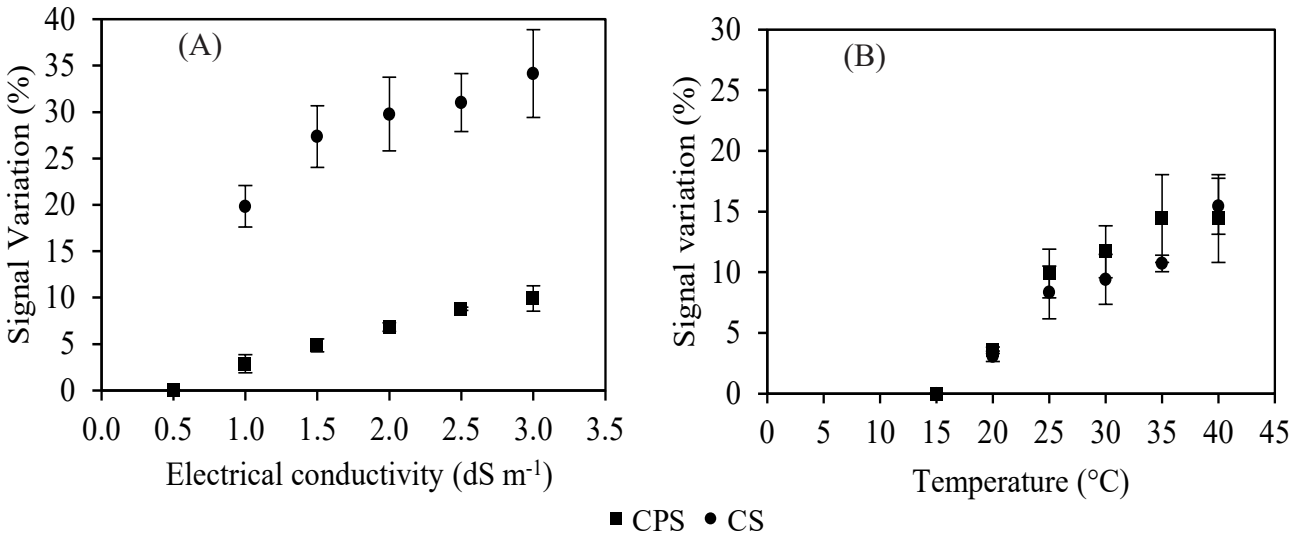

The variation in the EC of the medium due to the increase in the concentration of ions influences the dielectric constant, leading to an increase in the values of electrical permittivity and, consequently, capacitance (Evett *et al*., 2006). Therefore, due to the inverse relationship between "*f* and C", the increase in EC causes a decrease in frequency, overestimating soil moisture values. Zabolotnyi and Koshevoi (2020) observed overestimations in water content using capacitive sensors when changing the chemical properties of the solution used. When analyzing different capacitive probes, Bogena *et al*. (2007) and Evett *et al*. (2006) also observed overestimations in soil water content with an increase in the EC of the medium, attributing the observed variation to the frequency range in which these sensors operate. At frequencies below 100 MHz, errors in volumetric water content measurements reached 1.3% and 5.4% in soils with EC of 0.1 and 1.0 dS m^{-1}.

Developed sensors operate in frequency ranges below 1.0 MHz, considered by Bogena *et al*. (2007) susceptible to interference from the electrical permittivity of the medium in the sensor signal. These interferences influence dielectric constant measurements in porous media with similar water content but different EC. Furthermore, the presence of free ionic charges potentiates the Maxwell-Wagner (M-W) effect in sensors operating at frequencies between the kHz and MHz ranges (Chen; Or, 2006).

The dielectric properties in materials of heterogeneous composition are mainly determined by the volume of the component with the highest dielectric value, which in the case of soil is water. The increase in temperature influences the agitation of the ions in the water and, consequently, the electrical conductivity of the soil, enhancing the M-W effect. The increase in the M-W effect causes an increase in the dielectric permittivity of

Table 4 - Costs for manufacturing the sensor and a reading device

Material	Quantity sold	Value (US$)*	Quantity used	Unit price (US$)
		Sensor		
Fiberglass board (15 X 15)	1	5.38	0.2	1.08
555 Oscillator	1	0.33	1	0.33
Resistor	100	0.27	1	0.00
Capacitor	10	0.24	1	0.02
Sleeved cable - 3 ways (m)	1	1.01	1	1.01
Male P2 plug	1	0.45	1	0.45
Epoxy Resin + Hardener (kg)	1	41.32	0.03	1.24
Subtotal				4.13
		Reading device		
Arduino Mega 2560 board	1	34.12	1	34.12
16 x 2 LCD display	1	4.69	1	4.69
Female P2 plug	1	2.35	1	2.35
9 V battery adapter 9 V	1	0.45	1	0.45
Plastic box for electronic circuit (15 x 15 cm)	1	6.32	1	6.32
Subtotal				47.92
Total (Sensor + Reading device)				52.06

*quotation of 04/17/2024

the soil in low frequency measurements (Chen; Or, 2006). Topp *et al*. (1980) also mention that temperature is one of the factors that affect the dielectric constant of the soil.

Cost of materials for manufacturing the sensor

Table 4 presents the costs of the materials used to manufacture a capacitive sensor unit (CPS) and a signal reading device. The cost of the sensor is considered low and corresponds to 8.62% of the cost of the reading device, which can be used to manage the reading of numerous sensors.

CONCLUSIONS

1. The coplanar sensor performed satisfactorily in different soil/substrate materials, providing a small error in determining the water content in the soil (0.0178 cm^3 cm^{-3});
2. The developed sensor showed sensitivity to temperature similar to that of the commercial sensor, and lower sensitivity to salinity than the commercial sensor;
3. The proposed sensor combines a low-cost, easy-to-fabricate design with an automated data acquisition system, making it a promising alternative for soil water content monitoring.

ACKNOWLEDGMENTS

The authors would like to thank the Carlos Chagas Filho Foundation for Research Support in the State of Rio de Janeiro (FAPERJ) for the financial support (E-26/202.909/2018) and the National Council for Scientific and Technological Development (CNPq) for the scholarship granted (Process 133663/2020-5) and financial support (Process 310604/2018-4).

DATA AVAILABILITY STATEMENT

The research data is available only upon request to the corresponding author.

REFERENCES

BADAVATH, N. *et al*. Landslide susceptibility mapping for West-Jaintia Hills district, Meghalaya. **Sadhana**, v. 49, p. 1-19, 2024. https://doi.org/10.1007/s12046-023-02404-9

BOGENA, H. R. *et al*. Evaluation of a low-cost soil water content sensor for wireless network applications. **Journal of Hydrology**, v. 344, p. 32-42, 2007. https://doi.org/10.1016/j.jhydrol.2007.06.032

CARDENAS-LAILHACAR, B.; DUKES, M. D. Precision of soil moisture sensor irrigation controllers under field conditions. **Agricultural Water Management**, v. 97, p. 666-672, 2010. https://doi.org/10.1016/j.agwat.2010.01.009

CHEN, Y.; OR, D. Effects of Maxwell-Wagner polarization on soil complex dielectric permittivity under variable temperature and electrical conductivity. **Water Resource Research**, v. 42, n. 6, p. W06424, 2006. https://doi.org/10.1029/2005WR004590

DUARTE, E.; HERNANDEZ, A. A review on soil moisture dynamics monitoring in semi-arid ecosystems: methods, techniques, and tools applied at different scales. **Applied Sciences**, v. 14, p. 7677, 2024. https://doi.org/10.3390/app14177677

EVETT, S. R *et al*. Soil Profile Water Content Determination: Sensor Accuracy, Axial Response, Calibration, Temperature Dependence, and Precision. **Vadose Zone Journal**, v. 5, p. 894-907, 2006. https://doi.org/10.2136/vzj2005.0149

GOMES, F. H. F. *et al*. Calibration of a low-cost soil moisture sensor. **Revista Brasileira de Agricultura Irrigada**, v. 11, p. 1509-1516, 2017. https://doi.org/10.7127/rbai.v11n400605

HEISTERMANN, M. *et al*. Technical Note: Revisiting the general calibration of cosmic-ray neutron sensors to estimate soil water content. **Hydrology and Earth System Sciences**, v. 28, p. 989-1000, 2024. https://doi.org/10.5194/hess-28-989-2024

KAMIENSKI, C.; VISOLI, M. C. Swamp: a precision irrigation platform based on the internet of things. **Fonte,** v. 15, p. 76-84, 2018. https://ainfo.cnptia.embrapa.br/digital/bitstream/item/191516/1/AP-Swamp.pdf

LEONE, M. Advances in fiber optic sensors for soil moisture monitoring: a review. **Results in Optics**, v. 7, p. 100213, 2022. https://doi.org/10.1016/j.rio.2022.100213

LIU, Y. *et al*. A review of Earth's surface soil moisture retrieval models via remote sensing. **Water**, v. 15, p. 3757, 2023. https://doi.org/10.3390/w15213757

LO, T. H. *et al*. Field assessment of interreplicate variability from eight electromagnetic soil moisture sensors. **Agricultural Water Management**, v. 231, p. 105984, 2020. https://doi.org/10.1016/j.agwat.2019.105984

MORIASI, D. N. *et al*. Model evaluation guidelines for systematic quantification of accuracy in watershed simulations. **Transactions of the ASABE**, v. 50, p. 885-900, 2007. https://doi.org/10.13031/2013.23153

ODUOR, N. *et al*. Soil management strategies enhanced crop yield, soil moisture, and water productivity in Nitisols of the Upper Eastern Kenya. **Environmental Challenges**, v. 5, p. 100375, 2021. https://doi.org/10.1016/j.envc.2021.100375

OLIVEIRA, I. N. *et al*. Capacitance probe calibration for an Ultisol Udult cultivated with sugarcane by soil tillages. **Agricultural Water Management**, v. 241, p. 106341, 2020. https://doi.org/10.1016/j.agwat.2020.106341

PERTASSEK, T. *et al*. **Hyprop-fit Software User's Manual**. V.3.0, UMS GmbH. Version 3.0, München/Germany. 2015. 66 p.

PIZETTA, S. C. *et al*. Calibration of a capacitive sensor to estimate moisture in three classes of soil. **Irriga**, v. 22, p. 458-468, 2017. http://dx.doi.org/10.15809/irriga.2017v22n3p458-468

ROTH, K. *et al*. Calibration of Time Domain Reflectometry for Water Content Measurement Using a Composite Dielectric Approach. **Water Resources Research**, v. 26, p. 2267-2273, 1990. https://doi.org/10.1029/WR026i010p02267

ROTIMI, E. *et al*. Field Performance of Five Soil Moisture Instruments in Heavy Clay Soils. **Soil Science Society of America Journal**, v. 79, p. 20-29, 2015. https://doi.org/10.2136/sssaj2014.06.0250

SHARMA, H. *et al*. Soil moisture sensor calibration, actual evapotranspiration, and crop coefficients for drip irrigated greenhouse chile peppers. **Agricultural Water Management**, v. 179, p. 81-91, 2017. https://doi.org/10.1016/j.agwat.2016.07.001

SINGH, A. *et al*. Strategies to measure soil moisture using traditional methods, automated sensors, remote sensing, and machine learning techniques: review, bibliometric analysis, applications, research findings, and future directions. **IEEE Access**, v. 11, p. 13605-13635, 2023. https://doi.org/10.1109/ACCESS.2023.3243635

SINGH, J. *et al*. Performance assessment of factory and field calibrations for electromagnetic sensors in a loam soil. **Agricultural Water Management**, v. 196, p. 87-98, 2018. https://doi.org/10.1016/j.agwat.2017.10.020

SONGARA, J. C.; PATEL, J. N. Calibration and Comparison of Various Sensors for Soil Moisture Measurement. **Measurement**, v. 197, p. 11130, 2022. https://doi.org/10.1016/j.measurement.2022.111301

SZYPLOWSKA, A. *et al*. Dielectric models for moisture determination of soils with variable organic matter content. **Geoderma**, v. 401, p. 115288, 2021. https://doi.org/10.1016/j.geoderma.2021.115288

TOPP, G. C. *et al*. Electromagnetic determination of soil water content: Measurement in coaxial transmission lines. **Water Resources Research**, v. 16, p. 574-582, 1980. https://doi.org/10.1029/WR016i003p00574

VEREECKEN, H. *et al*. Soil hydrology in the Earth system. **Nature Reviews Earth & Environment**, v. 3, p. 573-587, 2022. https://doi.org/10.1038/s43017-022-00324-6

VERMA, S.; PAHUJA, R. Recalibration and performance comparison of soil moisture sensors using regression and neural network characteristic models. **Materials Today: Proceedings**, v. 45, p. 4852-4861, 2021. https://doi.org/10.1016/j.matpr.2021.01.306

VORIES, E.; SUDDUTH, K. Determining sensor-based field capacity for irrigation scheduling. **Agricultural Water Management**, v. 250, p. 106860, 2021. https://doi.org/10.1016/j.agwat.2021.106860

YU, H. *et al*. The agricultural planting structure adjustment based on water footprint and multi-objective optimization models in China. **Journal of Cleaner Production**, v. 297, p. 126646, 2021. https://doi.org/10.1016/j.jclepro.2021.126646

ZABOLOTNYI, O.; KOSHEVOI, M. An effective method of bulk materials moisture measurement using capacitive sensors. **Journal of Stored Products Research**, v. 89, p. 101733, 2020. https://doi.org/10.1016/j.jspr.2020.101733

ZENG, J. *et al*. Microwave remote sensing of soil moisture: current status and future perspectives. **Remote Sensing**, v. 15, n. 17, p. 4243, 2023. https://doi.org/10.3390/rs15174243

ZHANG, X. *et al*. Advanced technologies of soil moisture monitoring in precision agriculture: a review. **Journal of Agriculture and Food Research**, v. 18, e101473, 2024. https://doi.org/10.1016/j.jafr.2024.101473

This is an open-access article distributed under the terms of the Creative Commons Attribution License